

~~From MCM~~  
#75-26.4

PREDICTION OF AIR POLLUTION CONCENTRATIONS FROM AGRICULTURAL BURNING

ANDERS DANIELS AND WILFRID BACH

UNIVERSITY OF HAWAII  
HONOLULU, HAWAII

KARL HOW

HAWAII SUGAR PLANTERS ASSOCIATION  
HONOLULU, HAWAII



For Presentation at the 68th Annual Meeting of the

Air Pollution Control Association

Boston, Massachusetts

June 15-20, 1975

PREDICTION OF AIR POLLUTION CONCENTRATIONS  
FROM AGRICULTURAL BURNING

by

Anders Daniels and Wilfrid Bach  
University of Hawaii  
Honolulu, Hawaii 96822

and

Karl How  
Hawaii Sugar Planters Association  
Honolulu, Hawaii 96822

ABSTRACT: The body of information presented in this paper is directed to those interested in assessing emission rates and concentration levels from agricultural burning, and/or those interested in simulation techniques. This paper describes a source-oriented air pollution monitoring program for agricultural burning in Hawaii and presents a simulation technique for estimating field emission rates and ambient pollutant concentration levels. Several samplers were used to obtain a number of independent estimates of field emission rates. Although individual estimates showed considerable variation, the average calculated emission rate was close to that obtained from a burning tower test. The advantage of the simulation approach as compared to burning tower studies is that not only emission rates, but more importantly, ambient pollutant levels can be assessed.

NOTE TO EDITORS

Publication rights to this paper are reserved for the Journal of the Air Pollution Control Association. Any use by other journals is limited to twenty per cent of text and figures.

PREDICTION OF AIR POLLUTION CONCENTRATIONS  
FROM AGRICULTURAL BURNING

This study was undertaken to calculate the emission rates and to simulate concentration patterns of air pollutants from agricultural burning. In this paper we shall present the simulation technique used and shall illustrate the technique by considering particulate matter from one field burn.

Practice of Agricultural Burning in Hawaii

During the past three quarters of this century agricultural burning has been common practice in the Hawaiian Islands. Sugar cane fields are burned before harvesting. The crowns of pineapples are left in the field for drying and are subsequently burned. This burning practice reduces the bulk of material that is hauled to the processing plants. The burn also serves as rodent and insect control. The remaining ashes furthermore act as fertilizer

The disadvantage of the burning practice is that rather high levels of pollutant concentrations will be experienced downwind of a burn. A number of complaints have been voiced from residents in areas affected by burns.

Control Strategy

Mandated by the 1970 Clean Air Act, the Hawaii Department of Health (DOH) began a program to determine effects from agricultural burning. The control strategy for pollutants emitted by such fires was based on the proportional model. Since the input of this model consists only of emission rates, the control strategy of the DOH centered around the determination of such emission rates. This approach does, however, not consider actual concentrations, which are controlled by the ambient air quality standards.

Emission rates from agricultural burning can be determined by using the following two methods: laboratory burning tower tests and concentration simulation models. Both methods have their advantages and disadvantages. In a burning tower one can control the burn and make accurate emission estimates. But the question arises, how realistically can actual burn conditions be simulated? This is of particular importance for large area source burns, such as cane and pineapple fields. The simulation model technique is, on the other hand, based on actual concentration measurements in the field from which the overall concentration pattern can be extrapolated. Also effects of different weather situations can be simulated. Simulated emission rates are, however, more likely to show a larger variance than values obtained from controlled burning tower experiments.

At the time of implementation plan development, no emission data for cane and pineapple field burns were available. Therefore, a burning tower study was conducted by the Statewide Air Pollution Research Center, Riverside, California, for the EPA. (1) This study produced a mean particulate matter emission of 7.2 lb per ton of sugar cane burned. The standard deviation for the 15 experiments was 1.6 lb per ton.

Air Quality Simulation Study--Sampling

As a supplement to the burning tower experiments in California, an air quality sampling and simulation program for agricultural burning was initiated

in Hawaii. The major pollutants from agricultural burning are suspended particulates, carbon monoxide, and hydrocarbons. These pollutants were measured by high volume samplers, an NDIR analyzer, and a flame ionization analyzer. Fifteen high volume samplers were located at different distances in the predicted downwind direction of a fire. The gas samplers were located at the closest sampling point to the field. The arrangement of the samplers (Fig. 1) was dictated by the availability of cane roads. The samplers were operated during a burn which lasted about 30 minutes. To determine the background concentration the samplers were operated for another 30-minute period. The gas sampling was continuous during the entire period.

A station recording wind speed and direction was operating upwind at a height of 10 m above the ground. Wind direction variations were also recorded using an MRI sigma vane. Pilot balloon observations were also taken during a burn.

Aerial photos of the smoke were taken from an aircraft at about 3000 m. Vertical temperature profiles were also recorded during an ascent and a descent. A ground-based time lapse camera was operated several kilometers away from the burns. About 30 cane fires and 5 pineapple fires were investigated during the 1973 burning season.

Air Quality Sampling Study--Modeling

For the evaluation of the aerial smoke plume photos the height, tilt, and swing of the camera has to be determined. Two methods were used to determine the height: (1) altimeter heights were corrected for the actual lapse rate as measured by the temperature probe on the aircraft; and (2) heights were determined photogrammetrically from the distance between two known points on the photos and in nature. For the example which we shall use to illustrate our simulation technique, the independently estimated heights are within a few percent of each other. The tilt and swing of the camera's photo plane was determined by identifying three points on the photo and in nature. The swing was calculated with reference to a predetermined direction.

The ground-based distance between the ground camera and the fire was determined from a map. The relative heights of camera position and fire, and the relative position of the fire within the photo frame reference yield the camera position, tilt, and swing. The photos are then projected onto a screen and the visible outline of the smoke can then be drawn. Then a reference system is identified on the photos and the visible outline of the horizontal and vertical plume is measured within the reference frame in steps of 2.5 cm along the downwind axis.

The visible plume coordinates are then combined with camera and projector data (position, tilt, swing, focal length) to determine the visible plume outline points on a Cartesian coordinate system. An iterative process was employed between the areal and ground-based photos.

The projected visible plume outline points are then used to calculate second order logarithmic expressions for the horizontal and vertical plume widths using the method of least squares. In the present example the equations are:

$$\log a(x) = 0.10 (\log x)^2 - 0.17 \log x + 1.77 \quad (1)$$

and

$$\log b(x) = 0.055 (\log x)^2 + 0.116 \log x + 1.606 \quad (2)$$

where

- $x$  = the actually traveled downwind distance (m)  
 $a(x)$  = the vertical width of the plume (m)  
 $b(x)$  = the horizontal width of the plume at right angles to the plume axis (m)

It will later on be assumed that the smoke concentration in the plume is normally distributed, and therefore a knowledge of the vertical and horizontal standard deviations will be sufficient to determine the concentration at any point. It is furthermore assumed that the horizontal and vertical standard deviations also obey a second order logarithmic relationship.

Roberts' (2) opacity theory is used to determine the coefficients in the sigma expressions. This theory states that the same concentration contrast can be seen in both the horizontal and vertical smoke photos. It is assumed that the field can be approximated by the limited line source concept. Thus the concentrations at the horizontal and vertical edges of the plume are the same. This can mathematically be expressed as:

$$\chi(x_0, b(x_0), 0) = \frac{Q}{2\pi u \sigma_z^2(x_0)} \int_{-1}^1 \frac{\exp[-b^2(x_0)/2\sigma_y^2(x_0)]}{\sigma_y^2(x_0)^{21}} db =$$

$$\chi(x_0, 0, a(x_0)) = \frac{Q \exp[-a^2(x_0)/2\sigma_z^2(x_0)]}{2\pi u \sigma_y^2(x_0) \sigma_z^2(x_0)} \quad (3)$$

where

- $1$  = half the field width  
 $u$  = wind speed  
 $Q$  = emission rate  
 $\chi(x, y, z)$  = the concentration at  $x, y, z$

To determine the unknown coefficients in the expressions for the standard deviations  $\sigma_y$  and  $\sigma_z$  the concentrations at some ten downwind distances ( $x_0$ ) were calculated using an interactive technique and the method of least squares. In our example the expressions are:

$$\log \sigma_z(x) = 0.1 (\log x)^2 - 0.16 \log x + 1.64 \quad (4)$$

and

$$\log \sigma_y(x) = 0.045 (\log x)^2 + 0.183 \log x + 1.34 \quad (5)$$

Fig. 2 shows these expressions in comparison with the expressions in Turner's Workbook (3) for stability class C.

These expressions together with the coordinates for horizontal and vertical centerline points, and the vertical wind speed profile (from pibal observations) are then used as input for the simulation calculations.

The surface wind speed and direction record, sampler locations and operating times, field size, location, and burning time complete the input to the simulation model.

The model for agricultural burning, which will now be discussed, is basically a time-stepping modified limited Gaussian line source model. The first task in the modeling is to divide the field into a number of segments based on the surface wind records. These records are subdivided into a number of equally long periods for which the average wind speed and direction is determined. In our case the chosen time period was 1 minute ( $\Delta t$ ) giving 30 segments for a 30 minute burn. In general a burn is started at the downwind corner of a field. We assume that the burn rate is proportional to the component of the wind at right angle to the burning line ( $u_A$ ), i.e.

$$\text{burn rate} = k u_A \quad (6)$$

where  $k$  is some constant. This assumption seems to be reasonable, since the burn rate depends on the oxygen supply. Next the downwind and upwind corner of the field are connected with a line, and the component,  $k u_B$ , of the burn rate in the direction of this line is calculated. Thus the burned distance ( $d_i$ ) along this line during one time period  $\Delta t$  is

$$d_i = k u_B \Delta t \quad (7)$$

The total distance ( $D$ ) along this line is then measured on a map. Thus one can write:

$$D = \sum_{i=1}^N d_i \quad (8)$$

where  $N$  is the number of time periods during a burn. From Eq. (8)  $k$  is determined and the burn distances  $d_i$  are calculated.

Next the equations for straight lines connecting neighboring field corners are calculated in the coordinate system used in connection with the smoke photos. It is then assumed that the burn line propagates at right angle to the wind direction of the first period. The intersections of the burn line at the beginning and end of each burn period with the field perimeter then gives the coordinates for each burn segment.

Next we simulate the burn of the first field segment. At the end of this burn period the downwind points of the segment have moved downwind according to the wind field and the upwind corners are still at the original points. It is assumed that the vertical wind speed profile (as obtained from the pibal observation) and wind direction profile (as obtained from the smoke photos) remains constant during the burn, while the surface wind speed and direction varies in time (as obtained by the surface wind station). The position of the puff corners is calculated using finite differencing for five twenty second time steps (i.e., the corner position moves horizontally for 20 seconds with the wind at that height, for which the new height of the puff corner is calculated etc.). This procedure is repeated for the next one minute time step, and this process continues until the puff has traveled beyond the samplers. Then the second segment puff goes through the same procedure, followed by the third puff, until the last segment puff has passed over the last sampler. In Fig. 1 the positions of the rightmost and leftmost puffs are shown for each one minute time period. Also shown is the outline of the field and the locations of the samplers.

For each puff and time period the model determines, if a line at right angle to the wind direction experienced by the two last corner points of the puff through any sampler location intersects the puff. If this is the case the horizontal distance  $d_0$  the puff has traveled is inserted in Eq. (4) to calculate  $\sigma_z(d_0)$ . The height of the centerline  $H(d_0)$  is divided by this value of  $\sigma_z(d_0)$  yielding a ratio  $R = H(d_0)/\sigma_z(d_0)$ . This ratio thus corresponds to a certain fraction of the centerline concentration, and it is this fraction that the sampler measures. The mass of pollutants monitored by the surface sampler has not traveled along the centerline, and it therefore gives erroneous results, if the centerline is used as the pollutant trajectory. The actual trajectory for this mass of pollutants must therefore be calculated using the same procedure followed for the centerline, replacing, however, the height of the puff  $H(d)$  with the height  $H_T(d)$  at which the mass of pollutants actually travels, i.e.

$$H_T(d) = H(d) - R\sigma_z(d) \quad (9)$$

Now the simulation program goes back to the initial puff position and repeats the previous procedure only replacing the centerline height with the heights calculated in Eq. (9). This now results in new travel distances  $d_0$  for the sampled pollutants.

We next calculate the deposit (mass) on the filter paper at the sampler caused by the smoke of the puff which affects the sampler during the one minute period. The modeled concentration at the sampler resulting from this puff ( $X_i$ ) is:

$$X_i = \frac{Q_i}{2\pi\sigma_z(d_i) u_i 2l_i} \exp\left\{-1/2 \left(\frac{H(d_i)}{\sigma_z(d_i)}\right)^2\right\} \int_{-l_i}^{l_i} \exp\left\{-1/2 \left(\frac{y_i - y_{0i}}{\sigma_y(d_i)}\right)^2\right\} dy_i \quad (10)$$

where

- $Q_i$  = emission rate of the burning field in mass per time (M/t)
- $l_i$  = half the length of the  $i$ th field segment (L)
- $d_i$  = the recalculated travel distance of the  $i$ th puff (L)
- $u_i$  =  $d_i/n_i\Delta t$  where  $n_i$  is the number of time periods ( $\Delta t$ ) during which the puff has traveled (L/t)
- $H(d_i)$  = height of the puff centerline (L)
- $y_i - y_{0i}$  = the horizontal distance from the sampler to the centerline of the puff (L)

The emission rate  $Q_i$  can be written as

$$Q_i = \frac{E A_i}{\Delta t 2l_i} \quad (11)$$

where

- $E$  = the field emission in mass per area ( $M/L^2$ )
- $A_i$  = the area of the  $i$ th segment ( $L^2$ )

$X_i$  can now be written as:

$$X_i = \frac{E A_i n_i}{2l_i \sqrt{2\pi} \sigma_z(d_i) d_i} \exp\left\{-1/2 \left(\frac{H(d_i)}{\sigma_z(d_i)}\right)^2\right\} \left[ \phi\left(\frac{y_i - y_{0i}}{\sigma_y(d_i)}\right) - \phi\left(\frac{y_i + y_{0i}}{\sigma_y(d_i)}\right) \right] \quad (12)$$

where

$$\Phi(z) = \int_{-\infty}^z \exp\left\{-\left(\frac{g}{2}\right)/\sqrt{2\pi}\right\} dg$$

The deposited mass ( $m_i$ ) on the sampler from this puff is:

$$m_i = X_i \Delta t F \quad (13)$$

where

$$F = \text{flow rate of the sampler (M/L}^3\text{)}$$

The mass deposited by all puffs is therefore obtained by summing  $m_i$  over all puffs.

We must also include the effect of background pollution. By sampling prior or after a field burn and assuming that the background pollution levels remain unchanged, we can calculate the amount deposited on the sampler ( $M_B$ ) caused by background pollution ( $X_B$ ) as follows:

$$M_B = X_B(t_2 - t_1) F \quad (14)$$

where

$$t_2 - t_1 = \text{sampling time}$$

Thus, the total mass deposited ( $M$ ) on the sample is:

$$M = M_B + \sum_{i=1}^N m_i \quad (15)$$

where

$$N = \text{the number of puffs affecting the sampler.}$$

The calculated concentration at the location of the sampler is therefore

$$X_c = \frac{M}{F(t_2 - t_1)} \quad (16)$$

This calculated concentration ( $X_c$ ) is now set equal to the measured concentration ( $X_m$ ) and the equation is solved for the field emission ( $E$ ), the desired parameter.

$$E = \frac{(X_m - X_B) (t_2 - t_1)}{\Delta t \sum_{i=1}^N n_i (\phi_1 - \phi_2)_i A_i \exp - 1/2 \left( \frac{H (d_i)}{\sigma_z (d_i)} \right)^2} \quad (17)$$

$$\sqrt{2\pi} \sum_{i=1}^N \sigma_z (d_i) d_i$$

The field emission rate (E) was calculated independently for all samplers as shown in Table I which also include the measured concentrations during burn and no-burn periods.

#### Conclusions

Ideally the field emission rates as shown in Table I should be the same for each sampler. The variation in the emission rate from sampler to sampler is, however, quite substantial. Reasons for these discrepancies might be variations in the background concentrations during burn and no-burn periods, unrepresentative sampling locations imposed by the scarce road network, variation in topography, and human error during predawn burn hours. Errors and approximations in the data reduction procedures, and finite differencing in the model itself, also contribute to the variation in the emission rates between the samplers.

The average calculated emission rate from all samplers is 172 lb/acre. This figure compares favorably with results from the burning tower experiment which have a range from 6.2 lb/ton for low moisture content to 24.8 lb/ton for high moisture content (1). For an average bulk of 11.8 ton of sugar cane trash/acre (4) the calculate emission is 14.5 lb/ton for this burn. This seems to indicate that the burning tower experiments can realistically reproduce actual burn conditions. The major advantage of using the simulation modeling approach as compared to the burning tower procedure is that, beside calculating the emission rate, more importantly, one can also assess the ambient air pollutant concentrations from agricultural burning.

#### References

1. E. F. Darley: Air Pollution Emissions from Burning Sugar Cane and Pineapple from Hawaii. Special Report to the Emission Factors Unit, EPA, Research Triangle Park, N. C., Aug. 1974.
2. O. F. T. Roberts: "The theoretical scattering of smoke in a turbulent atmosphere," *Proc. Roy. Soc., A*, 104, p. 640, (1923).
3. D. B. Turner: Workbook of Atmospheric Dispersion Estimates, U. S. Department of HEW, Public Health Service, Consumer Protection and Env. Health Service, NAPCA, 1969.
4. A. M. Dollar: Net fuel values for sugar cane in Hawaii: Report of Department of Agriculture, State of Hawaii. 1973.

Table I Measured Concentrations and Calculated Emission Values from a Selected Cane Field Burn

Sampler Number	Concentration ( $\mu\text{g}/\text{m}^3$ ) Background during Burn		Calculated Emission (lb/acre)
1	728	2273	358
2	521	6556	1058
3	1026	2674	205
4	1843	2907	222
5	348	943	94
6	223	401	27
7	125	338	54
8	345	584	232
9	64	204	22
10	126	305	28
11	188	218	6
12	94	138	12
13	606	730	34
14	164	192	110
15	165	173	115
			172 average

## Illustrations

- Fig. 1 Computer simulation of the travel of two puffs during a burning of sugar cane field.
- Fig. 2 A comparison between the calculated  $\sigma_y, \sigma_z$  and Turner's  $\sigma_y, \sigma_z$  for class C stability.

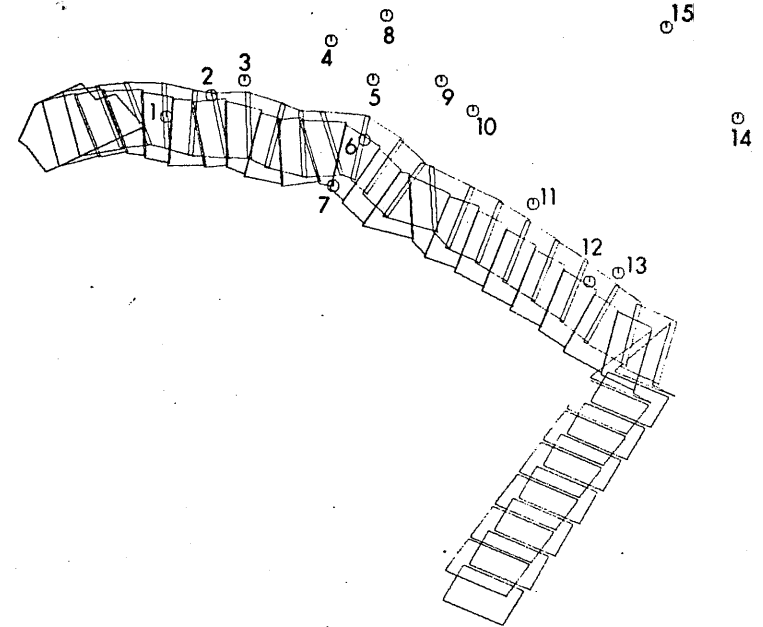


Fig. 1 Computer simulation of the travel of two puffs during a burning of sugar cane field.

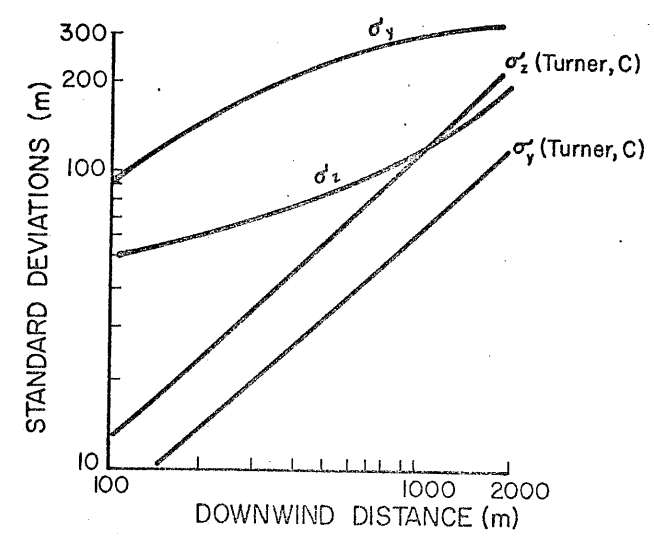


Fig. 2 A comparison between the calculated  $\sigma_y, \sigma_z$  and Turner's  $\sigma_y, \sigma_z$  for class C stability.